CONFERENCE PROCEEDINGS

Dynamics of CO_2 Plumes Encountering a Fault in a Reservoir

Kyung Won Chang, Steven L. Bryant

SIXTH ANNUAL CONFERENCE ON CARBON CAPTURE AND SEQUESTRATION - DOE/NETL
May 7 - 10, 2007

Abstract

After CO_2 has been injected in the lower part of a dipping aquifer, it will continue to migrate, driven by buoyancy. This movement drives a countercurrent flow of brine leading to increased residual phase trapping. The purpose of this simulation study is to understand the effects of geomechanical structures, especially faults, on the dynamic behavior of the buoyancy-driven CO_2 plume and the amount of residual trapping.

Using GEM (Generalized Equation-of-State Model Compositional Reservoir Simulator) we studied the behavior of CO_2 plumes (speed, direction, saturation at displacement front, residual phase trapping) in 2D formations with a range of fault properties (conductive vs. sealing, angle relative to dip, distance from initial plume location). We developed an analytical approach for estimating plume movement based on Buckley-Leverett theory, which compares favorably with the simulation results; thus, it can explain the basic behavior of CO_2 plume in this simplified reservoir model, which is homogeneous, anisotropic and tilted. Smaller amounts of initially stored CO_2 migrates shorter distances, and in these cases the simple theory predicts the plume movement prior to encountering a fault. If the plume encounters a fault within the reservoir, the fault can create new virtual source (CO_2 build-up at the plume/fault intersection) for migration. It also leads to more complicated fluid movement, including counter current flow. A sealing fault, which acts as another boundary for CO_2 plume, divides the aquifer into two parts: fault-independent zone and fault-dependent zone. The analytical solution can predict the properties of CO_2 plume in the first zone, but not in the latter one due to the counter current flow. In both cases of a declined and an inclined fault, CO_2 accumulates along the fault due to anisotropy causing dominantly parallel migration. The build-up continues until saturation approaches the endpoint dictated by the relative permeability curves (forming a virtual source),

and then CO_2 moves upward along the fault. On the other hand, a conductive fault, which acts as a new pathway for migration, may cause considerable leak of CO_2 toward the top boundary of the reservoir (inclined fault) or increase the width of CO_2 plume (declined fault). In the latter case of the conductive fault, the CO_2 plume passes through larger area, which improves the efficiency of residual saturation trapping. To understand the dynamics of CO_2 behavior, especially countercurrent flow, in the faulted reservoir we analyze flow vectors of both CO_2 and brine phases, which explain the process of gas build-up and/or leakage due to structural heterogeneity.

Introduction

Storage of carbon dioxide (CO_2) in a deep saline aquifer has been suggested as one method to reduce greenhouse gases in the atmosphere. Trapping and sealing CO_2 in deep brine formations underground requires a sufficiently impermeable caprock layer to prevent upward migration from the target reservoir. Accordingly, the risk of CO_2 leakage has been one of the main issues for CO_2 sequestration to be a reliable carbon dioxide management solution. However, caprock layers may contain imperfections, especially faults, which can act as a high-permeability conduit for leakage of CO_2 from depth to the near surface. Faults also pass through the target formations for storage. A fault can separate a formation into non-communicating compartments, or it can establish a conductive path to a juxtaposed but different formation.

The main purpose of this simulation study is to evaluate geometric (slope and angle) and/or petrophysical factors mainly associated with a fault, which should be taken into account in estimating the behavior of CO_2 plumes during carbon dioxide sequestration process. In addition, our works apply the following petrophysical concerns to the simulation model

containing each specific type of a fault: 1) anisotropy and isotropy of permeability; 2) residual gas saturation (residual saturation trapping); and 3) high-permeable portion in the sealing fault (leakage). Many CO_2 sequestration studies have done to explain the impact of the above three factors, but little attention has been paid to how the interaction between those factors and a fault affects the dynamics of CO_2 plumes. Therefore, in this simulation study we explore 1) how a fault within the storage formation affects the buoyancy-driven CO_2 migration, and 2) how the permanent capture of CO_2 can be increased from residual trapping mechanism in a fault-containing reservoir.

Description of the Simulation Model

The base case simulation presents results for the following domain: a relatively short, wide domain, of dimensions 400 ft (length) $\times$ 100 ft (height) $\times$ 2 ft (width), to establish a wide volume of CO_2 migration along which instabilities could develop. The simulation used 10,000 grid blocks; and, each grid block size is 2 ft $\times$ 2 ft $\times$ 2 ft. The aquifer was tilted at a dip angle of five degrees. In addition, there are no injection and production wells; the boundaries of the domain are closed. Accordingly, CO_2 migration is driven only by buoyancy. The intention is to study only the interaction with faults after injection has ended. Thus, this initial condition mimics the result of an "inject low and let rise" strategy. CO_2 is placed at high saturation in the lower part of the downdip half of the domain (range of the area is 1^{st} to 100^{th} grid block in j-direction (horizontal) and 40^{th} to 50^{th} grid block in k-direction (vertical)). The scheme of the base model is shown as the following Figure 1, and Table 1 summarizes input parameters including aquifer properties, component properties and well conditions. We use the GEM-CMG simulator

(Nghiem et al., 2004), tuned to the CO2/brine/rock system in previous work (Kumar et al., 2004; Ozah et al., 2005; Bryant et al., 2006).

The gas saturation profiles during 10,000 years are the principal simulation outputs to represent the dynamics of CO_2 plumes. The increase and/or decrease of the gas saturation in each grid block result from the phase behavior based on the relative permeability curve, which is introduced in Figure 2. The curve can be calculated from following relationships:

$$k_{rg} = k'_{rg}\left(\frac{S_g - S_{gcr}}{1 - S_{wcon} - S_{wir}}\right)^{N_g} \quad \text{for } S_g \geq S_{gcr}$$

$$k_{rw} = k'_{rw}\left(1 - \frac{S_g - S_{gr}}{1 - S_{wcon} - S_{gr}}\right)^{N_w} \quad \text{for } S_g \leq 1\text{-}S_{wcon}$$

$$k_{rg} = 0 \quad \text{for } S_g < S_{gcr}$$

$$k_{rw} = 0 \quad \text{for } S_g > 1\text{-}S_{wcon}$$

To analyze the effect of the residual gas saturation we use two comparative relative permeability curves including: 1) no residual gas saturation and 2) hysteresis with residual gas saturation.

Fault Properties

The CO_2 migration in a faulted reservoir was simulated by adding the petrophysical properties associated with fault characteristics. Such a geological discontinuity can induce the flow (leakage) of "potentially mobile CO_2" in the structural trap at large saturation. In the process of the structural trap, the stored CO_2 will remain in the trap permanently as long as the geological seal remains intact.

We represent faults by assigning appropriate transmissibility multipliers on every contact face of each grid block that would correspond to the prescribed location of a fault. The specific

range of grid blocks should be combined with fault parameters to represent fault properties; therefore, smaller grid blocks are required to simulate more realistically the angled geologic discontinuity. We categorize two types of a fault by geometry: declined (negative dip to horizontal plane) and inclined (positive dip to horizontal plane) fault. Also, the petrophysical characteristics of a fault: high-permeability (conduits) or low-permeability (barriers), can be controlled by setting transmissibility multipliers high (value over 1) or low (zero value). We can also model the presence of a local leak within a sealing fault by adjusting the transmissibility multiplier value of a specific grid block along the fault zone.

Analytical Solution for Buoyant Flow in Anisotropic Domain

Consider the flow of two immiscible fluids (one wetting and another non-wetting phase) in a homogeneous, isothermal and isotropic porous medium. The governing equation for the flow of phase *i* is from Darcy's law as follows:

$$\mathrm{u_i} = -\frac{\mathrm{k}\mathrm{k_{ri}}}{\mu_\mathrm{i}}\left(\frac{\mathrm{dp}}{\mathrm{dx}} + \rho_\mathrm{i}\mathrm{g}\,sin\,\alpha\right)$$

This simulation study focuses on the immiscible displacement only between two phases: gas (CO_2) and water (brine). Also, the reservoir model is based on two-dimensional domain; thus, it requires analyzing flow parallel to the bedding plane and vertical (Chang, 2007):

$$\mathrm{u_{g,parallel}} = \frac{\mathrm{k}\left(\rho_\mathrm{w} - \rho_\mathrm{g}\right)\mathrm{g}\,sin\,\alpha}{\frac{\mu_\mathrm{w}}{\mathrm{k_{rw}}} + \frac{\mu_\mathrm{g}}{\mathrm{k_{rg}}}}$$

$$\mathrm{u_{g,vertical}} = \frac{\mathrm{k}\left(\rho_\mathrm{w} - \rho_\mathrm{g}\right)\mathrm{g}\,sin\,90^\circ}{\frac{\mu_\mathrm{w}}{\mathrm{k_{rw}}} + \frac{\mu_\mathrm{g}}{\mathrm{k_{rg}}}} = \frac{\mathrm{k}\left(\rho_\mathrm{w} - \rho_\mathrm{g}\right)\mathrm{g}}{\frac{\mu_\mathrm{w}}{\mathrm{k_{rw}}} + \frac{\mu_\mathrm{g}}{\mathrm{k_{rg}}}}$$

The flux can be referred to the Darcy velocity of fluid, which represents its rates of flow per unit of surface at right angles to the direction of flow. The Darcy velocity differs from the interstitial velocity (v_g) of fluid because of the action of porosity and saturation:

$$u_g = v_g S_g \phi$$

Then, the distance and direction of CO_2 migration can be estimated as follows:

1) Distance

$$d_g = v_{total} \cdot t$$

$$v_{total} = \sqrt{v_{g,parallel}^2 + v_{g,vertical}^2 - 2v_{g,parallel} v_{g,vertical} \cos\left(90^\circ + \alpha\right)}$$

2) Angle

$$\theta = \cos^{-1}\left(\frac{v_{total}^2 + v_{parallel}^2 - v_{vertical}^2}{2v_{total} v_{parallel}}\right)$$

Simulation Results

Base Case

We first consider behavior in an aquifer containing no fault. The base model is assumed to be homogeneous and tilted. The only variable is vertical to horizontal permeability ratio (k_v/k_h) and the values are varied with 1 and 0.01. The first case represents the isotropic condition (k_v/k_h=1), which shows dominantly vertical movement of CO_2 plumes in spite of dipping condition. CO_2 plumes reach the top seal and spread out along the top boundary of the aquifer before approaching the side boundary. On the other hand, as the value of k_v/k_h becomes smaller, CO_2 migrates more parallel to the bedding plane in the up-dip direction. Accordingly, the lower k_v/k_h values are more efficient for storage of CO_2 gas. (Figure 3 and Figure 4)

The analytical estimation (angle and distance of movement) is quite reasonable to adapt Buckle-Leverett theory in analyzing the CO_2 plume behavior (Table 2). The agreement is remarkable, because the countercurrent flow exists at the edge of plumes except the frontal part. This violates the premises of Buckley-Leverett theory.

Effects of Fault Properties

The existence of a fault plays a significant role in controlling the CO_2 behavior corresponding to its geometric and petrophysical properties.

Geometric variables for a fault are location, angle and slope. In this simulation, every fault type bisects the domain by locating in the middle of the aquifer from 1st (top) to 50th (bottom) layers. Plus, all faults are placed at 45 degrees from the bottom of the aquifer. The declined fault contains a negative slope to the plane; while, the inclined fault has a positive slope. To represent petrophysical properties of a fault, transmissibility multiplier are used: zero (GEM code, *TRANSF*=0 and *IDIR*+/-, *JDIR*+/- and *KDIR*+/-) for the sealing (low-permeable) fault and 100 for the conductive (high-permeable) fault (*TRANSF*=100 and *IDIR*-, *JDIR*- and *KDIR*+/-). The simulation results for four distinct cases are categorized as follows:

1) Declined and Sealing Fault

First, the simulation work focuses on how the declined fault, which has negative slope corresponding to the dip of bedding plane, affects CO_2 migration under the anisotropic reservoir condition. The ration of vertical permeability to horizontal permeability is 0.01; thus, the flow parallel to the bedding plane will be greater than the vertical movement.

The declined fault plays a significant role as one of typical geological traps (Figure 5). In this case, the sealing fault forms a CO_2-trap-zone combined with the pre-existing boundaries of

an aquifer such as the top seal and side boundaries. Furthermore, from the above series of gas saturation profiles, the most remarkable phenomenon is the accumulation of CO_2 at the fault before the vertical CO_2 migration along the sealing fault. In detail, the flow vector analysis indicates there would be countercurrent flow between phases inside the CO_2 plume. Countercurrent flow means that applying the Buckley-Leverett theory (Buckley and Leverett, 1942) can not be valid to interpret the flow model during the process of CO_2 build-up.

2) Inclined and Sealing Fault

In the case of an inclined fault, the sealing fault cannot act as a geological trap; instead, it alters the path of the CO_2 migration (or leakage). In this simulation, the fault divides the CO_2-rich area into two parts, which induce separated behaviors of CO_2 plume. As Figure 6 shows, the left part (behind portion) of stored CO_2 moves upward along the sealing fault and then accumulates at the upper part of given reservoir. On the other hand, CO_2 plume in the right part (frontal portion) has a normal trend of fluid migration, which is observed from outputs of the base case as Figure 3. If the reservoir has smaller anisotropy or isotropy of permeability, we can expect that CO_2 of the left side will show a preferential movement toward the upper boundary as shown in Figure 4; while, CO_2 in the right side will migrate along the sealing fault.

3) Declined and Conductive Fault

Faults can provide channels for basement fluids to move across laterally continuous barriers to vertical fluid migration. The structural deformation of rocks during faulting and folding can enhance permeability with open joints, which exhibit only opening displacement. Higher transmissibility multiplier values (*TRANSF*=100) allow a specific series of grid blocks with inclination to represent high-permeable fault characteristics. This assumed fault can affect CO_2 migration as a conduit (so-called "channeling effect").

As shown in Figure 7, CO_2 does not accumulate in the fault zone, which means that the gas phase flows quickly across the fault due to relatively larger transfer capacity of the fault. CO_2 migration did not occur along the fault zone because the reservoir properties (anisotropy and dipping) have a great effect on the flow of the gas phase. As a result, despite the conductive fault property, CO_2 propagation tends to be parallel to the bedding plane not aligned to the fault zone. However, we can discover CO_2 buildup on the other side of a fault, which can be a virtual source for another CO_2 migration. It enlarges the contact area of CO_2 invasion so that the efficiency of residual saturation trapping will be increased.

4) Inclined and Conductive Fault

Through the outputs (Figure 8) from the inclined fault simulation we can discover that CO_2 flows dominantly through the conductive fault, and accumulates at the top seal of the aquifer. This phenomenon is exactly what we expected in the case of the conductive fault property, which can be regarded as "CO_2 leakage." (Figure 8) In addition, the conductive fault zone creates additional virtual sources of CO_2 along the fault. The combination of the dipping of the reservoir and the conductive fault geometry allows more residual CO_2 trapping by enlarging the contact area of the migration. In contrast to the previous case (declined fault model), the geometry of the fault (inclined condition) interplays with the petrophysical properties of the fault zone; and, positively affects CO_2 migration through the large-transfer-capacity geologic channel.

Residual Saturation Trapping

As CO_2 migrates through the formation, some of it is captured and permanently remained in the pore space, which is referred to "residual CO_2 trapping" (Obdam *et al.*, 2003). When the rate of

this trapping is relatively high and CO_2 is injected at the bottom of a sufficiently thick formation, almost all of the injected CO_2 can be trapped by the mechanism before it reaches the surface boundary of the formation. Likewise, the residual trapping mechanism plays a significant role in capturing CO_2 to be immobile.

From the simulation results (shown in Figure 9), we can easily figure out that all of grid blocks which CO_2 passes though show residual gas saturation: the blue color indicates 0.2 of gas saturation, which is the value of residual gas saturation, S_{gr}. Consequently, this case represents quite similar trend of CO_2 primarily-upward migration compared with the base case due to isotropic condition; however, the explicit difference is that CO_2 cannot reach the upper surface of the reservoir.

Flow Vector Analysis

For analyzing the dynamics of each phase we add flow vectors on the gas saturation profile. These show when and where the imbibition and/or drainage take place.

From Figure 10 through 11, we can discover counter current flow boundaries of the CO_2 plume except the propagating portion. Before CO_2 meets a fault, its lateral migration is controlled by counter current flows of the water phase. Once a fault begins to affect CO_2 migration, the behavior of CO_2 plume is controlled mainly by fault properties. In addition, counter current flows are detected inside the CO_2 plume, which means that CO_2 trapping can be enhanced by the counter current flow due to fault geometry.

The simulation results reveal that before CO_2 encounters a fault, counter current flow of brine exists inside CO_2 plume, but after hitting the fault, it disappears gradually in the region corresponding to the build-up saturation. On the contrary, counter current flow persists outside

CO_2 plume except the head of the plume at any migration step. This fact implies that counter current flow due to anisotropy (small value of k_v/k_h) results in parallel-dominant migration; but, the presence of a fault controls the dynamics of CO_2 behavior more than any other factors.

Conclusions

This study concludes that the properties of a fault and the interactions between the fault and the reservoir matrix can play a critical role in quantifying the behavior of CO_2 after injection ends. A fault within the target formation can have a positive or negative effect on the capture of the buoyancy-driven CO_2 with residual trapping mechanism depending on its geometry and/or petrophysical property. In addition, the counter current flow of water phase inside CO_2 plumes provides benefits to CO_2 trapping. Accordingly, when it comes to the injection and storage of CO_2, an accurate prediction of the fault conductivity and petrophysical properties of the reservoir would be required to optimize the rate of injection and the storage capacity of the reservoir for the permanent capture of CO_2.

Acknowledgements

This simulation works are performed at CPGE (Center for Petroleum and Geosystems Engineering) of the University of Texas at Austin. Plus, this project is supported by CCP2 (CO_2 Capture Project 2) and the Geologic CO_2 Storage Joint Industry Project. The members of the JIP include Chevron, ENI, ExxonMobil, Shell, TXU and Computer Modeling Group, Ltd.

Nomenclature

k_v vertical permeability

k_h horizontal permeability

k_{rg} relative permeability for gas phase

k_{rg}' gas end point relative permeability

k_{rw} relative permeability for water phase

k_{rw}' water end relative permeability

S_g gas saturation

S_{gcr} critical gas saturation

S_{gr} residual gas saturation

S_w water saturation

S_{wcon} connate water saturation

S_{wir} irreducible water saturation

N_g gas relative permeability exponent

N_w water relative permeability exponent

α dip angle (positive for upward flow)

u flux

μ viscosity

ρ density

g gravitational acceleration

v interstitial velocity

ϕ porosity

t total

References

1. Bryant, S.L. *et al.*: "Buoyancy-Dominated Multiphase Flow and Its Impact on Geological Sequestration," paper SPE 99938 presented at SPE/DOE Symp. Improved Oil Recovery, Tulsa, 22-26 Apr. 2006
2. Buckley, S.E. and Leverett, M.C., "Mechanism of Fluid Displacement in Sands," Trans. A.I.M.E.; Vol. 146; pp107-116, 1942
3. Chang, K., "A Simulation Study of Injected CO_2 Migration in the Faulted Zone," thesis; the University of Texas at Austin, 2007
4. Collins, R.E., "Flow of Fluids through Porous Materials," published by Penn-Well Pub. Co., Tulsa, OK; pp142-149, 1961
5. Kumar A. *et al.*: "Reservoir Simulation of CO_2 Storage in Deep Saline Aquifers," paper SPE 89343 presented at SPE/DOE 14th Symp. Improved Oil Recovery, Tulsa, 17-21 Apr. 2004
6. Main, I.G. *et al.*: "Fault Sealing during deformation-band growth in porous sandstone," Geology, Vol. 28; No. 12; pp1131-1134, Dec. 2000.
7. Manzocchi, T. *et al.*: "Fault transmissibility multipliers for flow simulation models," Petroleum Geoscience, Vol. 5; pp53-63, 1999
8. Nghiem, L., Sammon, P., Grabenstetter, J. and Ohkuma, H., "Modeling CO2 Storage in Aquifers with a Fully-Coupled Geochemical EOS Compositional Simulator," paper SPE 89474 presented at the 2004 SPE/DOE 14th Symp. on Improved Oil Recovery, Tulsa, OK, April 17-21, 2004
9. Pasala, S.M. *et al.*: "Simulating the Impact of Faults on CO_2 Sequestration and Enhanced Oil Recovery in Sandstone Aquifers," paper SPE 84186 presented at SPE ATCE, Denver, 5-8 October. 2003

10. Obdam, A., L.G.H. Van der Meer, May, F., Bech, N., Kervevan, C., and Wildenberg, A., "Effective CO_2 Storage Capacity in Aquifers and in Hydrocarbon Fields," 6th International Conference on Greenhouse Gas Control Technologies; Vol.I; pp.489-494, Kyoto, Japan, 2002

11. Ozah, R.C. *et al*.: "Numerical Simulation of the Storage of Pure CO_2 and CO_2-H_2S Gas Mixture in Deep Saline Aquifers," paper SPE 97255 presented at SPE ATCE, Dallas, 9-12 October. 2005

12. Pruess, K., "Numerical Studies of Fluid Leakage from a Geologic Disposal Reservoir for CO_2 Show Self-Limiting Feedback between Fluid Flow and Heat Transfer," Geophysical Research Letter; Vol.32; No. L14404; doi:10.1029, June 2005

13. Walsh, N.P. *et al.*: "An Analysis of Gravity-Dominated, Immiscible Flows in Dipping Reservoirs," paper SPE 21651 presented at Symp. Production Operations, Oklahoma City, 7-9 Apr. 1991

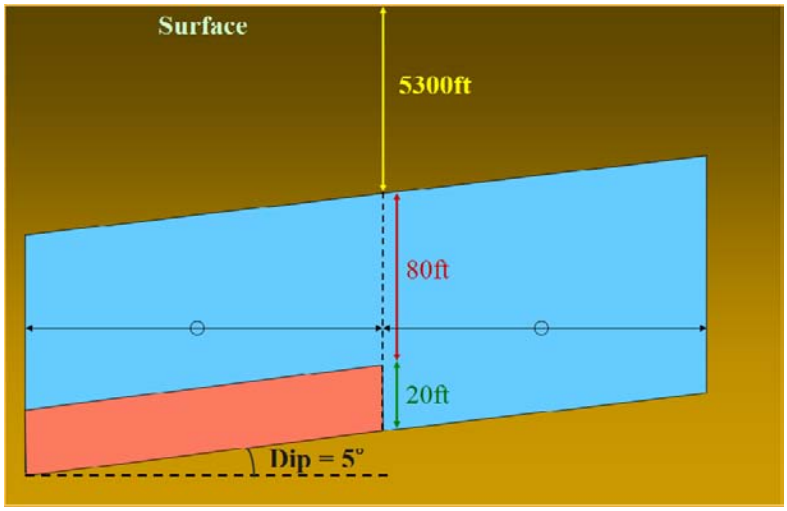

Figure 1: The scheme of base model for this simulation; the red color indicates the initial CO_2 location and the blue color represents the H_2O saturated zone.

General Property of Whole Aquifer	
Width, ft	400
Thickness, ft	100
Depth at top of the center of the reservoir, ft	5300
Temperature, degF	140
Salinity, ppm	100,000
Initial pressure at 5300 ft depth, psi	2295
Constant boundary pressure, psi	2295
Specific Property	Matrix
Permeability, md	1
Horizontal to vertical permeability ratio	1
Transmissibility	1
Horizontal to vertical transmissibility ratio	1
Porosity, fraction	0.15

Table 1: General Properties of the Reservoir Model

	Analytical Solution		Simulation Output	
k_v/k_h	Distance, ft	Angle, deg	Distance, ft	Angle, deg
0.01	122.55	6.46	123.27	4.63
0.1	57.38	46.09	57.52	41.15
1	34.9756	80.08	27.88	77

Table 2: Quantities Comparison of Analytical Solution and Simulation Output

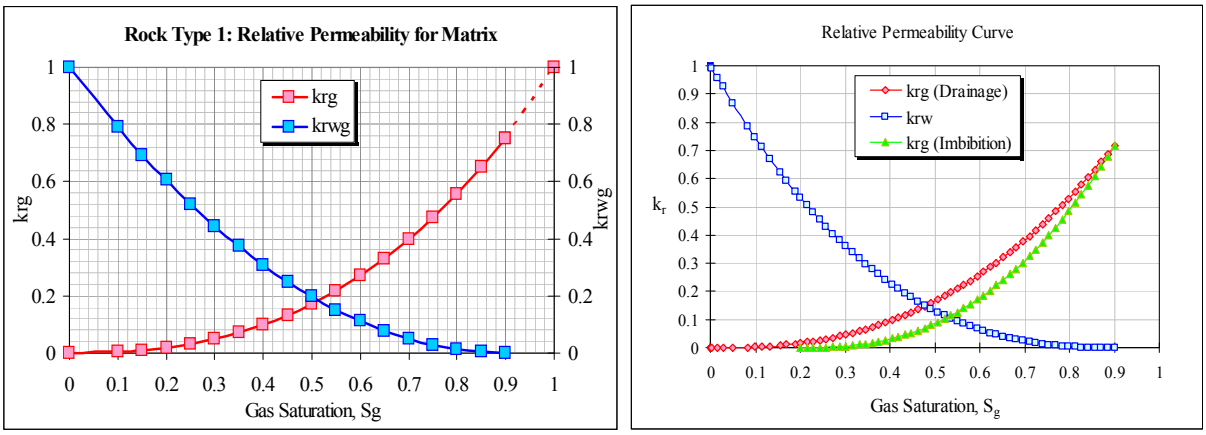

Figure 2: Relative permeability curves: the first one does not contain residual gas saturation, while the second one involves residual gas saturation (S_{gr}=0.2) by using hysteresis

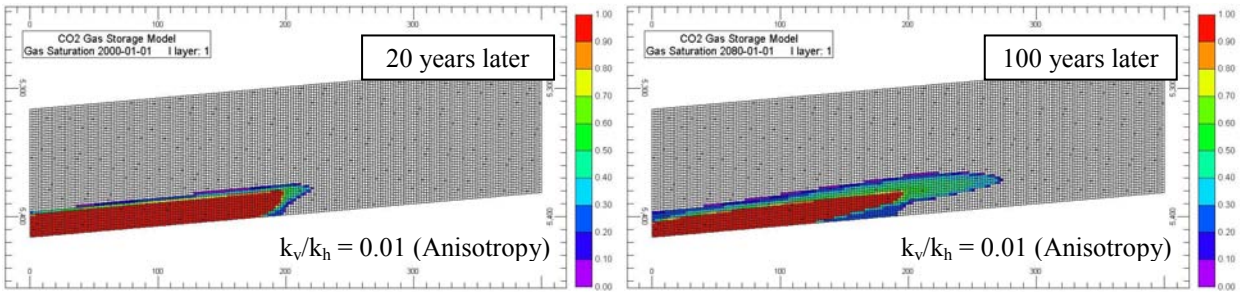

Figure 3: The gas saturation profiles after 20 years and 100years; the aquifer involves 0.2 of residual gas saturation and anisotropic permeability (k_v/k_h=0.01)

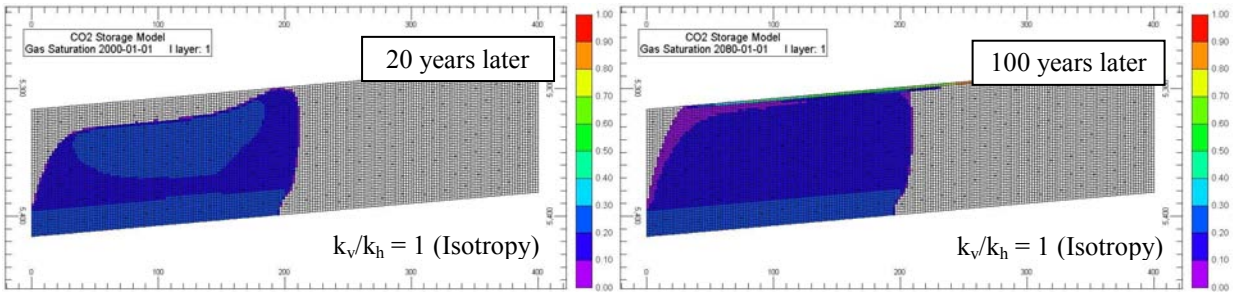

Figure 4: The gas saturation profiles after 20 years and 100years; the aquifer involves 0.2 of the residual gas saturation and isotropic permeability (k_v/k_h=1)

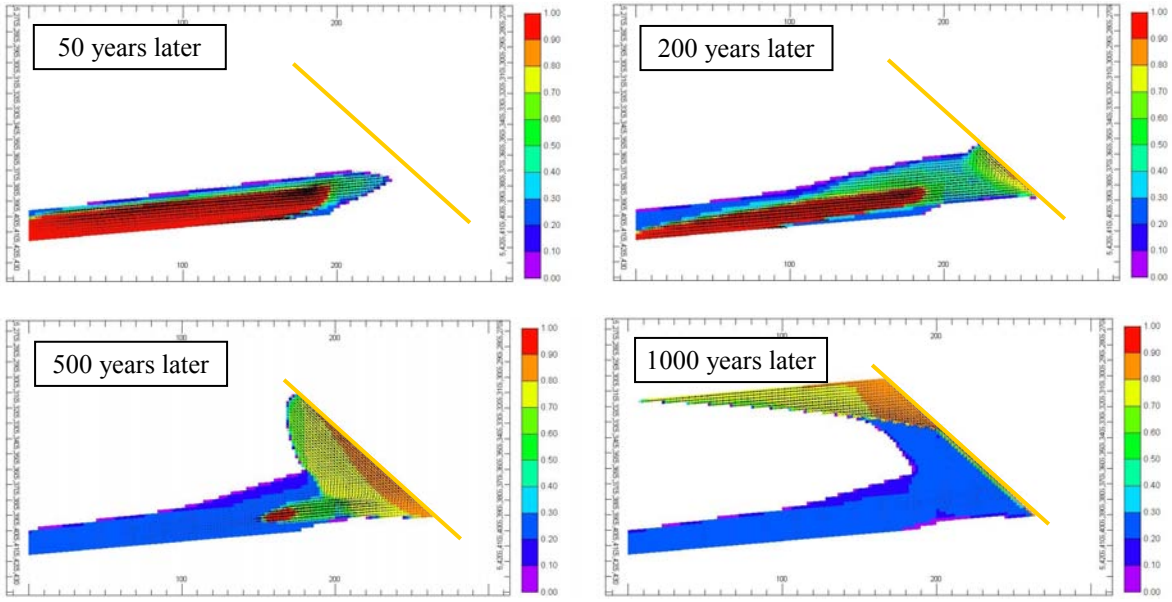

Figure 5: Gas saturation profiles for declined and sealing (low-permeable) fault; the model contains anisotropy (k_v/k_h=0.01) and residual gas saturation (S_{gr}=0.2); the yellow line represents the fault.

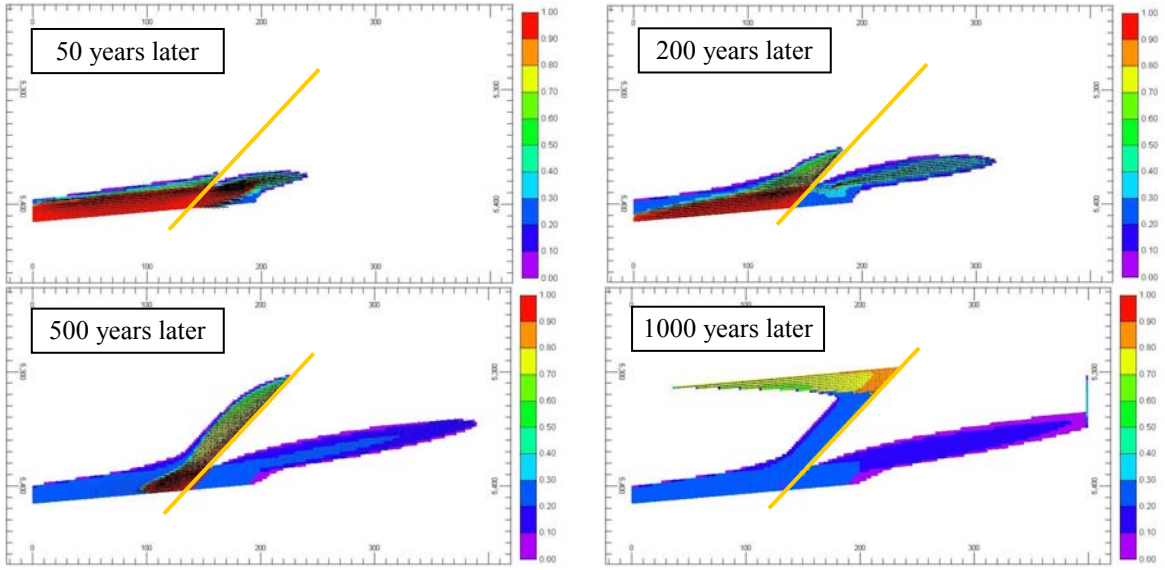

Figure 6: Gas saturation profiles for inclined and sealing (low-permeable) fault; the model contains anisotropy (k_v/k_h=0.01) and residual gas saturation (S_{gr}=0.2); the yellow line represents the fault.

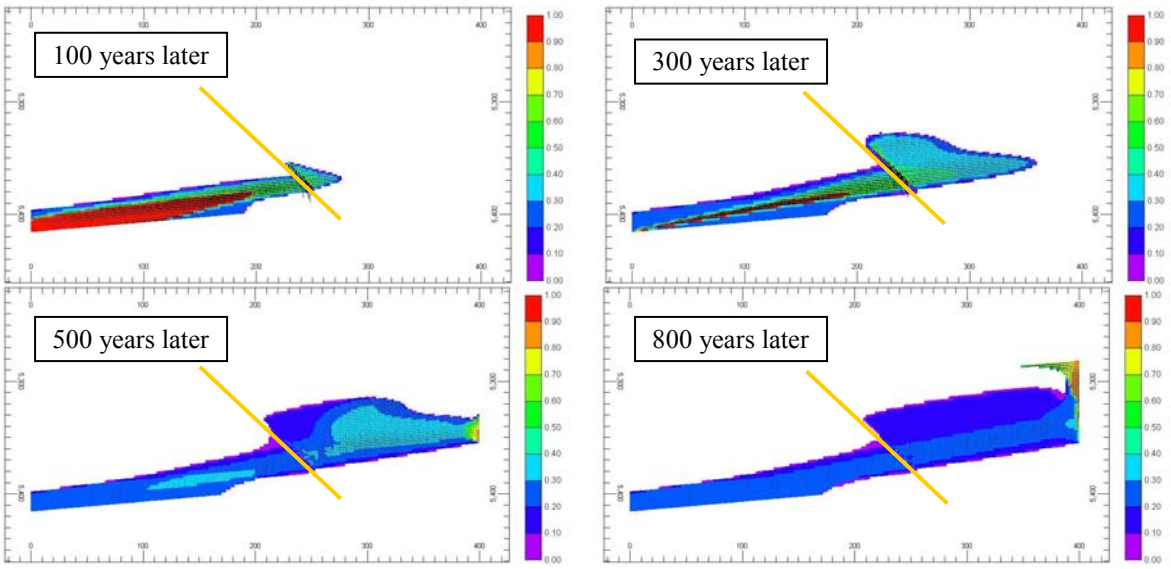

Figure 7: Gas saturation profiles for declined and conductive (high-permeable) fault; the model contains anisotropy (k_v/k_h=0.01) and residual gas saturation (S_{gr}=0.2); the yellow line represents the fault

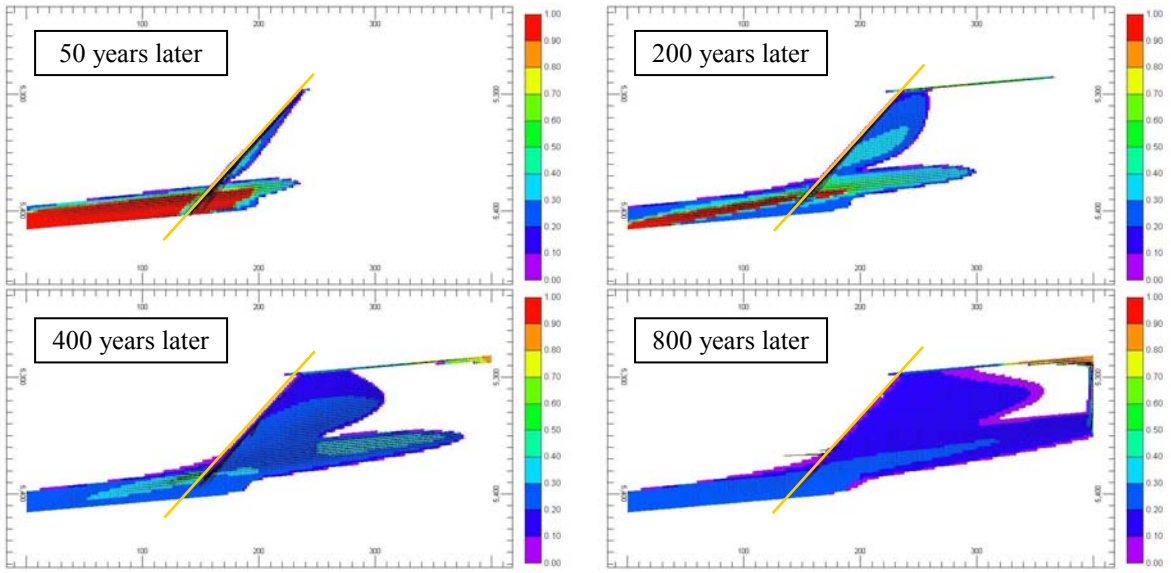

Figure 8: Gas saturation profiles for inclined and conductive (high-permeable) fault; the model contains anisotropy (k_v/k_h=0.01) and residual gas saturation (S_{gr}=0.2); the yellow line represents the fault

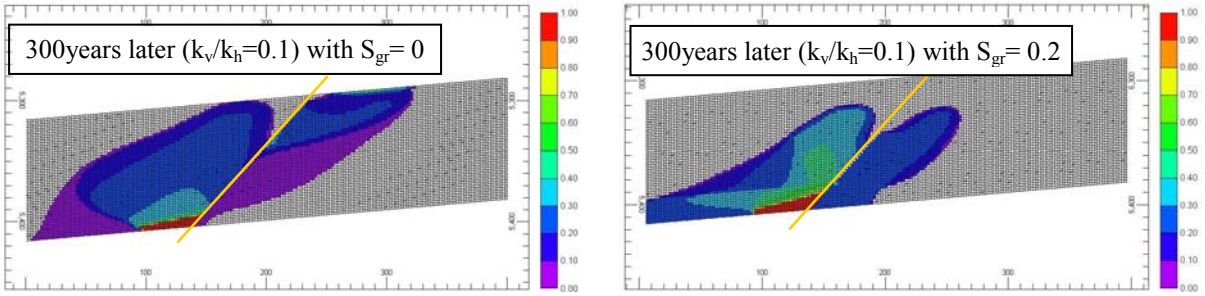

Figure 9: Gas saturation profiles for revealing the effect of residual gas saturation; the fault is inclined and sealing; the yellow line represents the fault

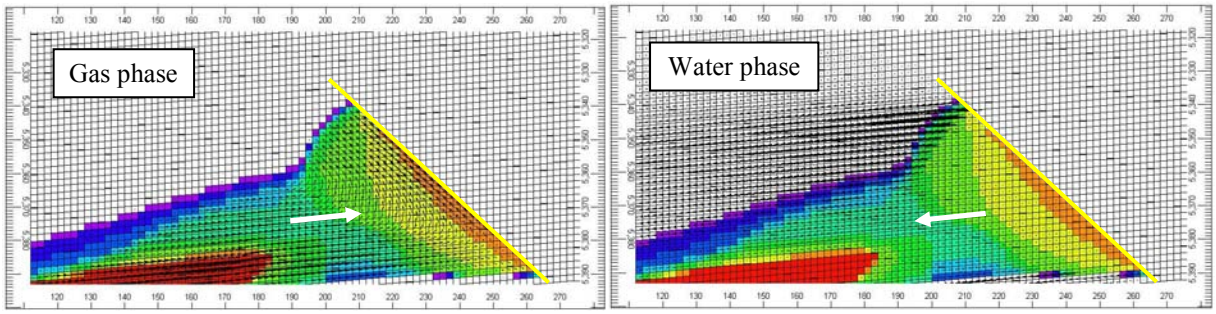

Figure 10: Gas saturation profiles with flow vectors to analyze the dynamics of CO_2 plumes of the model involving declined and sealing fault; the white arrows represent the major direction of phase vectors; the yellow line represents the fault

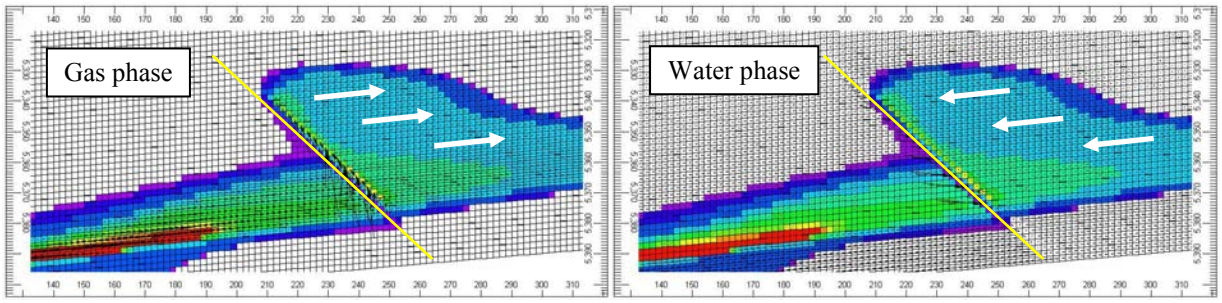

Figure 11: Gas saturation profiles with flow vectors to analyze the dynamics of CO_2 plumes of the model involving inclined and conductive fault; the white arrows represent the major direction of phase vectors; the yellow line represents the fault